

## FY2020 FES Theory Milestone

### “Modeling of Fully 3D Vertical Displacement Event Disruptions”

First quarterly Progress report – Dec 31, 2019

Prepared by: Stephen C. Jardin, PPPL, Carl Sovinec, U. Wisconsin, Madison

**Summary:** The proposed first quarter FY20 milestone was: “Perform and document benchmark M3D-C1/NIMROD 2D VDE calculations in simplified geometry”. This has been completed and a paper has been submitted to Physics of Plasmas. In addition to benchmarking NIMROD and M3D-C1, a team representing the European MHD code JOREK asked to be included in the benchmark activity, and so we have successfully performed a 3-way benchmark between these 3 codes: M3D-C1, NIMROD, and JOREK. The benchmark problems include determining the linear growth rate as a function of the wall resistivity, determining the growth rates from the linear phase of a nonlinear calculation, and comparing the time-dependent trajectories of the magnetic axis ( $R, Z$ ), the toroidal current, the induced wall current, and the halo current and its distribution. The agreement obtained between the axisymmetric results from the three codes provides confidence in our preprocessing methods, normalizations, and algorithms when moving to the 3D phase of the benchmark.

#### 1. Introduction

A Vertical Displacement Event (VDE) is an off-normal occurrence in a tokamak in which position control of the discharge is lost, and the tokamak plasma moves rapidly upward or downward until it makes contact with the vacuum vessel. The discharge current in ITER will be up to 15 MA. When a plasma with this current makes contact with the vessel, it will induce large currents into the metallic vessel, and these currents will cause large forces. Previous studies commissioned by ITER to calculate these forces assumed that the plasma remained axisymmetric during the VDE to simplify the calculation. However, it is known that the plasma column will deform and produce "sideways forces" in ITER [1] that could potentially damage the machine. Our two flagship MHD codes, NIMROD [2] and M3D-C1 [3,4] now have the capability of modeling a fully 3D plasma interacting with a conducting structure. We plan to use this capability to realistically model a full 3D VDE in ITER and to calculate the expected forces. In this first quarter we have performed an axisymmetric (2D) benchmark of NIMROD and M3D-C1, as well as the European code JOREK [5,6].

#### 2. Problem Setup

The equilibrium used for this benchmark case is loosely based on the NSTX discharge #139536 at  $t = 309$  ms. It is illustrated in Fig. 1. An axisymmetric rectangular resistive wall is used to simplify the geometry. The corners of the inner boundary of the resistive wall domain are at  $(R = 0.24 \text{ m}, Z = \pm 1.4 \text{ m})$  and  $(R = 1.6 \text{ m}, Z = \pm 1.4 \text{ m})$ . The thickness of the resistive wall is set to  $\Delta_w = 0.015 \text{ m}$ .

The equilibrium position of the magnetic axis is  $(R_{\text{axis}} = 1.07 \text{ m}, Z_{\text{axis}} = -0.015 \text{ m})$ . The toroidal magnetic field on axis is  $B_{\text{tor}} = 0.37 \text{ T}$ , the total toroidal plasma current is  $I_{\text{tot}} = 5.7 \cdot 10^5 \text{ A}$ . The difference between the poloidal magnetic flux at the boundary and at the magnetic axis is  $\Psi_{\text{bnd}} - \Psi_{\text{axis}} = -0.059 \text{ Vs}$ , where  $\Psi = - \int B_{\text{pol}} dA / 2\pi$ . The temperature profile is given by  $T_e(\Psi) = 1 \text{ keV} \cdot (\rho(\Psi) / \rho_{\text{axis}})^{0.6}$ . The pressure and current density profiles are defined in the *geqdsk equilibrium* file.

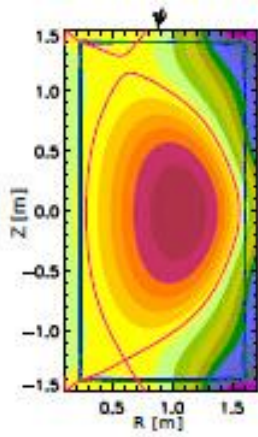


**Figure 1. Equilibrium poloidal magnetic flux of the VDE benchmark case (M3D-C1). Also shown are the separatrix (red line) and the resistive wall (green and blue lines). The plasma equilibrium came from a reconstruction of NSTX discharge #139536. However the vessel (resistive wall) is not the NSTX vacuum vessel, but rather a rectangular shaped axisy**

Dynamic viscosity, perpendicular and parallel heat diffusion coefficients and the particle diffusion coefficient are constant in space and time. Their values are given by  $\nu = 5.16 \cdot 10^{-6} \text{ kg}(\text{ms})^{-1}$ ,  $\kappa_{\perp} = 1.54 \cdot 10^{19} (\text{ms})^{-1}$ ,  $\kappa_{\parallel} = 10^5 \kappa_{\perp}$ ,  $D_n = 1.54 \cdot 10^{-1} \text{ m}^2 \text{ s}^{-1}$ ,  $T_{e,\text{edge}} = 14.65 \text{ eV}$  (section 3),  $= 1 \text{ eV}$  (section 4). The plasma resistivity is given by the Spitzer model (i.e.  $\eta(T_e) = 1.03 \cdot 10^{-4} \cdot Z \cdot \ln \Lambda \cdot (T_e[\text{eV}])^{-3/2} \Omega \text{ m}$ , where  $Z = 1$ ,  $\ln \Lambda = 17$ ). The ion mass is set to twice the proton mass. A loop voltage is not applied.

### 3. Linear Results

For simulations with JOEK that include a resistive wall, the JOEK-STARWALL coupling is used [6,7]. Similar to NIMROD and in contrast to M3D-C<sup>1</sup>, JOEK uses a spectral representation for the toroidal discretization. Cubic Bézier finite elements are used for the discretization in the  $R$ - $Z$  plane. There are a few differences between the model that JOEK uses for the benchmark simulations and the models that M3D-C<sup>1</sup> and NIMROD use: (i) Although JOEK has a full MHD option, it uses a reduced MHD model [8] for the VDE calculations presented here since the JOEK-STARWALL coupling is not yet available for the full MHD model. (ii) In JOEK-STARWALL, the vacuum contribution is implemented by using a Green's function method. Therefore, it is not necessary to discretize the vacuum region and apply ideal wall boundary conditions in an outer boundary. This property comes from the fact that the full vacuum response can be expressed as a function of the magnetic field at the plasma boundary. (iii) At the resistive wall, instead of no-slip boundary conditions, only the normal component of the velocity vanishes.

For the JOEK simulations presented here, a polar grid is used with increase resolution in the region surrounding the point of contact between plasma and wall. Since JOEK does not have an option that allows linear simulations with toroidal mode number  $n = 0$ , we compare the VDE growth rates in the early, linear phase of the evolution obtained in 2D axisymmetric nonlinear simulations.

In order to be able to run benchmark cases in the regime where the VDE growth rate is not influenced by response currents in the open field line region, the value of the edge temperature has to be sufficiently small. Since in nonlinear simulations too small values of the edge temperature can lead to numerical problems, we use a small temperature offset only within the calculation of the Spitzer resistivity such that  $\eta(T_e) = \eta_{\text{Spitzer}}(T_e - T_{e,\text{off}})$  in all three codes. Here, the edge temperature is  $T_{e,\text{edge}} =$

14.65 eV and the offset is  $T_{e,off} = 13.65$  eV which results in an effective edge resistivity corresponding to a temperature of  $T_{e,eff} = 1$  eV. For simplicity, the Ohmic heating term in the temperature equation is switched off.

Figure 2 shows a comparison of the resulting VDE growth rates. They have been obtained from the 2D nonlinear simulations by fitting  $Z_{axis} = a + b \cdot \exp(\gamma t)$  to the time trace of the vertical position of the magnetic axis where  $\gamma$  is the growth rate. Only the early, linear phase of the evolution (vertical position of magnetic axis between  $Z_{axis} = -1.64$  cm and  $Z_{axis} = -3.04$  cm) has been taken into account.

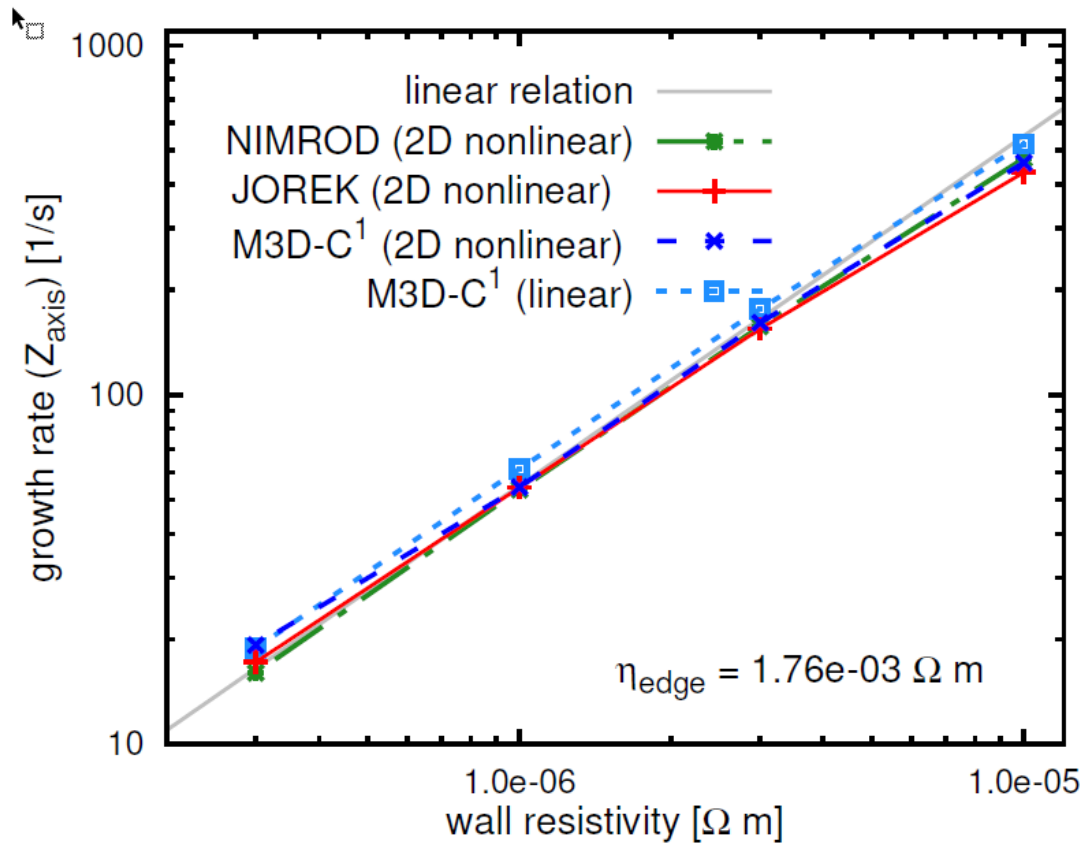


Figure 2. Comparison of VDE growth rates from the linear phase of 2D nonlinear M3D-C1, NIMROD and JOREK simulations. They deviate between 0.3% and 15%. Also shown are the results of linear M3D-C1 calculations.

All three codes find the expected linear relation between VDE growth rate and wall resistivity and the results agree well. The deviation between the obtained growth rates is around 3% or less for most wall resistivities and does not exceed 12% in the other cases, except for a deviation of 15% between the M3D-C<sup>1</sup> and the NIMROD result for the smallest wall resistivity. Also the growth rates obtained from linear M3D-C<sup>1</sup> simulations agree well with the results from the early phase of the 2D nonlinear simulations. However, it should be noted that such good agreement between the growth rates obtained from the linear and the nonlinear simulations is only achieved when the simulation

is first run in 2D nonlinear mode for a few time steps (in this case until the plasma has drifted by  $\sim 2$  mm), and then restarted as a linear simulation. A possible reason for this might be small inconsistencies in the geqdsk equilibrium that relax quickly when run in nonlinear mode. The exact cause for this will need some further investigation.

#### 4. Non-Linear Results

In the following, the results obtained by JOREK, NIMROD and M3D-C<sup>1</sup> on the further axisymmetric nonlinear evolution of a VDE are compared. The set up and parameters of these simulations are the same as for the simulations discussed in Section 3, except that  $T_{e,off} = 0$  such that the edge resistivity corresponds to an edge electron temperature of  $T_{e,edge} = 14.65$  eV. The resistivity of the wall has been set to  $\eta_w = 3 \cdot 10^{-6} \Omega \text{ m}$ .

In addition, a thermal quench has been artificially initiated during the course of the evolution. In 3D nonlinear MHD simulations, e.g. [9], the decrease of the edge safety factor during the course of a VDE causes non-axisymmetric instabilities to develop. These 3D instabilities cause the magnetic flux surfaces to break up which leads to greatly increased thermal transport. Since this effect cannot occur in axisymmetric simulations, an artificial thermal quench is initiated by increasing the perpendicular heat diffusion coefficient by a factor of 500 when the plasma becomes limited by the wall. Also, the particle diffusion coefficient is multiplied by a factor of 20.

The poloidal magnetic flux at the point in time when the plasma becomes limited by the wall in the M3D-C<sup>1</sup> simulation and the time traces of the thermal energy in the M3D-C<sup>1</sup>, JOREK and NIMROD simulation are shown in Figs. 3 and 4.

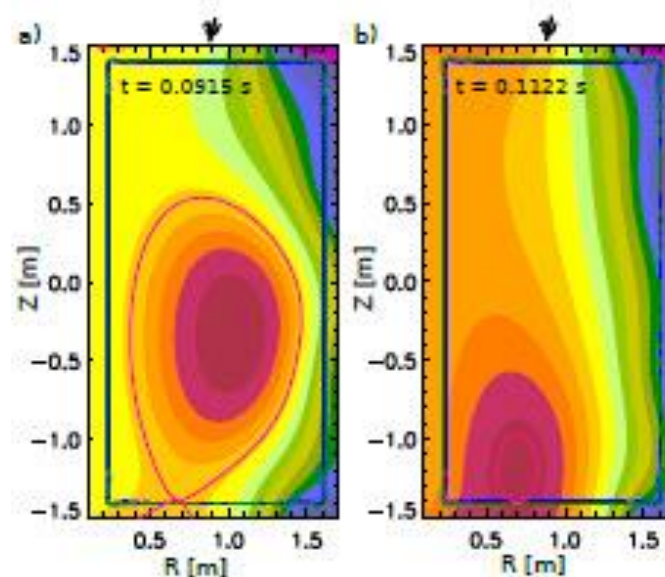
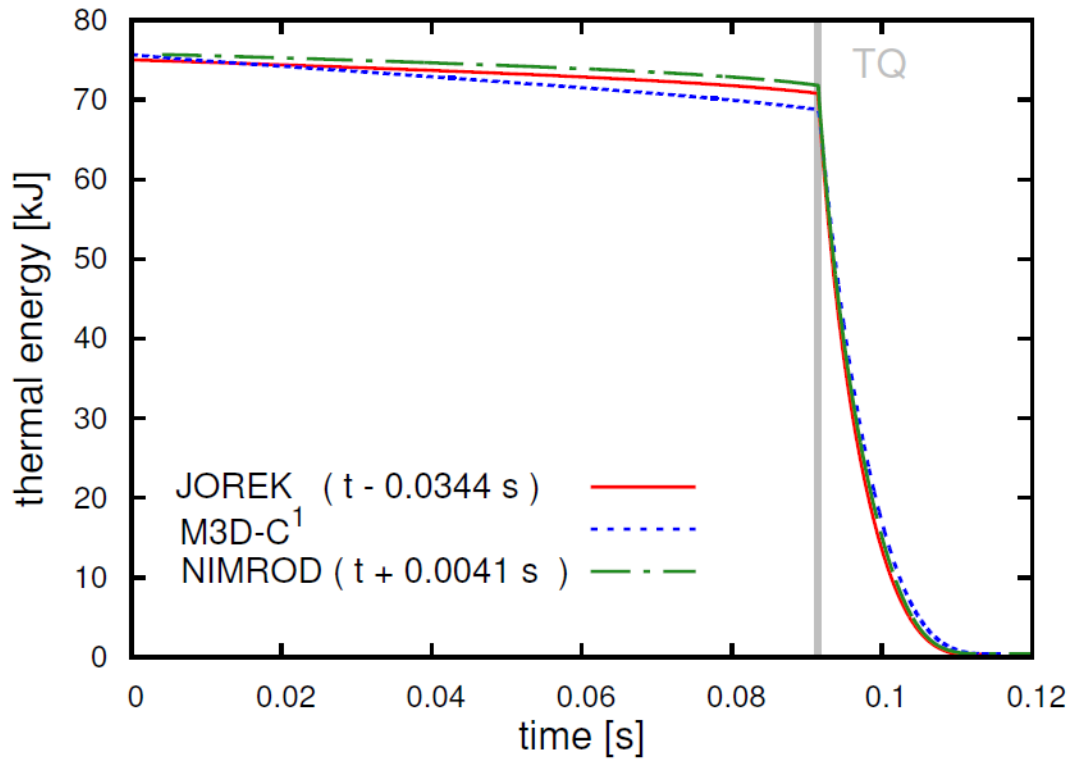


Figure 3 Contour plots show the poloidal magnetic flux in the 2D nonlinear M3D-C1 simulation at the point in time when the plasma first becomes limited by the wall (a) and close to the end of the VDE (b).



**Figure 4:** The time traces of the thermal energy in the M3D-C1, NIMROD and JOREK simulation show the artificial thermal quench initiated when the plasma touches the wall ( $t = 0.0915$  s for M3D-C1; JOREK and NIMROD traces have been shifted in time such that the points in time of the first plasma-wall contact coincide).

In order to enable a meaningful comparison of the results, the signals are slightly shifted in time such that the points in time of the first plasma-wall contact, e.g. the start of the thermal quench, coincide. This compensates for differences caused by the exponential dependency on the initial conditions. (The plasma first touches the wall at  $t \approx 126$  ms in the JOREK simulation, at  $t \approx 87.4$  ms in the NIMROD simulation and at  $t \approx 91.5$  ms in the M3D-C simulation.) Fig. 5 compares the time traces of the vertical and radial positions of the magnetic axis, the toroidal current enclosed by the last closed flux surface (LCFS), the total toroidal current inside the LCFS and in the open field line region and the net toroidal current in the resistive wall. (The NIMROD time traces in Figs. 5 d) and e) are missing because NIMROD does not currently have the corresponding diagnostics.)

In addition, the halo current at the plasma-wall interface, i.e. the component of the current density perpendicular to the wall at the wall, is shown for a point in time during the late evolution (when  $Z_{\text{axis}} \approx -1.23$  m). The halo current is plotted against the distance along the wall, measured counter-clockwise, starting at the low-field side midplane. For the JOREK simulation, the halo current is calculated from  $\mathbf{j} \times \mathbf{B} = \nabla p$ , assuming that the plasma is in equilibrium. Note that the location of the halo current spikes resulting from the M3D-C<sup>1</sup> simulation appears to be slightly shifted with respect to the other two traces. This is an artefact caused by the M3D-C<sup>1</sup> resistive wall having a slightly larger circumference since its corners are less rounded than the ones of the resistive walls used for the JOREK and NIMROD simulations.

As expected, the halo current flows into and out of the wall in a narrow region surrounding the contact point of the last closed flux surface and the wall. Despite the differences in physics models and numerical implementation between the three codes, the results agree well.

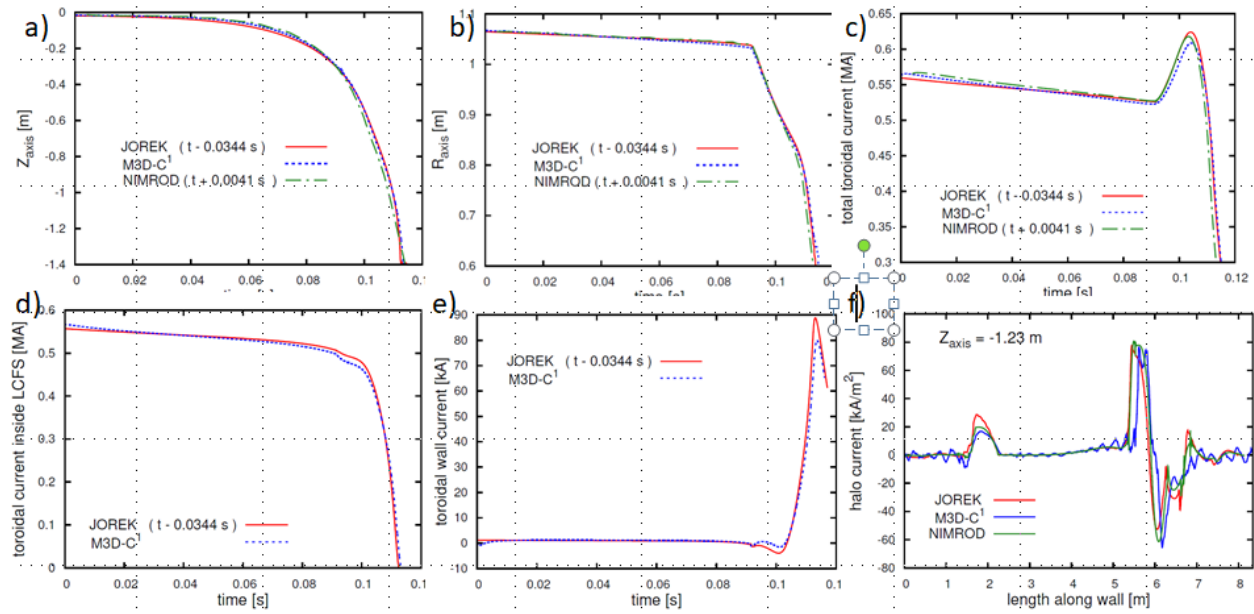


**Figure 5: Comparison of time traces from a 2D nonlinear simulation performed with JOREK, NIMROD and M3D-C<sup>1</sup>:** a) vertical position of magnetic axis, b) radial position of magnetic axis, c) toroidal current inside the LCFS and the open field line region, d) toroidal current inside the LCFS, e) net toroidal wall current. JOREK and NIMROD time traces are shifted so that the points in time of the first plasma-wall contact coincide. f) shows the component of the current density that is normal to the wall traced along the length along the wall at the point in time when  $Z_{\text{axis}} = -1.23$  m. The trace starts at the low-field side midplane and continues counterclockwise.

## 5. Summary

NIMROD and M3D-C1, as well as the European MHD code JOREK, have performed an axisymmetric VDE calculation with the same problem specifications and compared results. The results for the linear growth rates as well as for the nonlinear evolution are in excellent agreement. These calculations and their documentation here and in a article submitted to the Physics of Plasmas successfully meets the 1<sup>st</sup> quarter milestone for FY2020.

## Acknowledgments

The calculations documented here were carried out by I. Krebs ( PPPL and FOM Institute DIFFER – Dutch Institute for Fundamental Energy Research), C. Sovinec and K. Bunkers (University of Wisconsin, Madison), F. J. Artola (ITER Organization), M. Hoelzl (Max Plank Institute for Plasma Physics), and N. Ferraro, C. Clauser and S. Jardin (PPPL). This work was supported by US DOE Contracts No. DE-AC02-09CH11466 and No. DE-SC0018001, and the SciDAC Center for Tokamak Transient Simulations. Some of the computations presented in this report used resources of the National Energy Research Scientific Computing Center (NERSC), a U.S. Department of Energy Office of Science User Facility operated under Contract No. DE-AC02-05CH11231. The support from the EUROfusion Researcher Fellowship programme under the task agreement WP19-20-ERG-DIFFER/Krebs is gratefully acknowledged. Part of this work has been carried out within the framework of the EUROfusion Consortium and has received funding from the Euratom research

and training programme 2014-2018 and 2019-2020 under grant agreement No 633053. The views and opinions expressed herein do not necessarily reflect those of the European Commission.

## References

- [1] T. Schioler, C. Bachmann, G. Mazzone, and G. Sannazzaro, "Dynamic response of the ITER tokamak during asymmetric VDEs," *Fusion Engineering and Design*, . **86**, pp. 1963–1966, 2011.
- [2] C. R. Sovinec, A. H. Glasser, T. A. Gianakon, D. C. Barnes, R. A. Nebel, S. E. Kruger, D. D. Schnack, S. J. Plimpton, A. Tarditi, M. S. Chu, and the NIMROD Team, "Nonlinear magnetohydrodynamics simulation using high-order finite elements," *Journal of Computational Physics*, **195**, pp. 355–386, 2004.
- [3] S. C. Jardin, N. Ferraro, J. Breslau, and J. Chen, "Multiple timescale calculations of sawteeth and other global macroscopic dynamics of tokamak plasmas," *Computational Science & Discovery*, **5**, p. 014002, 2012
- [4] N. M. Ferraro, S. C. Jardin, L. L. Lao, M. S. Shephard, and F. Zhang, "Multi-region approach to free-boundary three-dimensional tokamak equilibria and resistive wall instabilities," *Physics of Plasmas*, v**23**, p. 056114, 2016.
- [5] G. Huysmans and O. Czarny, "MHD stability in x-point geometry: simulation of ELMs," *Nuclear fusion*, **47**, p. 659, 2007.
- [6] M. Hoelzl, P. Merkel, G. Huysmans, E. Nardon, E. Strumberger, R. McAdams, I. Chapman, S. Günter, and K. Lackner, "Coupling JOREK and STARWALL codes for non-linear resistive- wall simulations," in *Journal of Physics: Conference Series*, **401**, p. 012010, IOP Publishing, 2012.
- [7] P. Merkel and E. Strumberger, "Linear MHD stability studies with the STARWALL code," *arXiv:1508.04911*, 2015.
- [8] G. Huysmans, S. Pamela, E. Van Der Plas, and P. Ramet, "Non-linear MHD simulations of edge localized modes (ELMs)," *Plasma Physics and Controlled Fusion*, **51**, 124012, 2009.
- [9] D. Pfefferlé, N. Ferraro, S. C. Jardin, I. Krebs, and A. Bhattacharjee, "Modelling of NSTX hot vertical displacement events using M3D-C1," *Physics of Plasmas*, . **25**, p056106, 2018

